Equivalent Lumped Elements G, L, C, and Unloaded Q's of Closed- and Open-Loop Ring Resonators

Lung-Hwa Hsieh, *Student Member, IEEE,* and Kai Chang, *Fellow, IEEE*

***Abstract*—A transmission-line model is used to extract the equivalent lumped-element circuits for the closed- and open-loop ring resonators. The unloaded Q's of the ring resonators can be calculated from the equivalent lumped elements G, L, and C. Four different configurations of microstrip ring resonators fabricated on low and high dielectric-constant substrates are used to investigate the lumped elements and unloaded Q's. The largest difference between the measured and calculated unloaded Q is 5.7%, which is due to measurement uncertainties and accuracies of the calculation. These simple expressions introduce an easy method for analyzing ring resonators in filters and provide, for the first time, a means of predicting their unloaded Q.**

***Index Terms*—Equivalent lumped elements, ring resonator, transmission-line model, unloaded Q.**

I. Introduction

FOR THE PAST three decades, the microstrip ring resonator has been widely utilized to measure effective dielectric constant, dispersion, and discontinuity parameters and to determine optimum substrate thickness [1]–[4]. Beyond measurement applications, the microstrip ring resonator has also been used in filters, oscillators, mixers, and antennas [5] because of its advantages of compact size, easy fabrication, narrow passband bandwidth, and low radiation loss. Recently, interesting compact filters using microstrip ring resonators for cellular and other mobile communication systems have been reported [6], [7].

The basic operation of the ring resonator based on the magnetic wall model was originally introduced by Wolff and Knoppik [2]. In addition, a simple mode chart of the ring was developed to describe the relation between the physical ring radius and resonant mode and frequency [8]. Although the mode chart of the magnetic wall model has been studied extensively, it provides only a limited description of the effects of the circuit parameters and dimensions [5]. A further study on a ring resonator using the transmission-line model was proposed [9]. The transmission-line model used a T-network in terms of equivalent impedances to analyze a ring circuit. However, this model showed a complex expression for the ring circuit. Another distributed-circuit model using cascaded transmission-line segments for a ring was reported [10]. The model can easily incorporate any discontinuities and solid-state devices along the ring. Although this model could predict the behavior of a ring resonator well, it could not provide a straightforward circuit view such as equivalent lumped elements G, L, and C for the ring circuit.

Manuscript received December 9, 2000.

The authors are with the Department of Electrical Engineering, Texas A&M University, College Station, TX 77843-3128 USA.

Publisher Item Identifier S 0018-9480(02)01155-9.

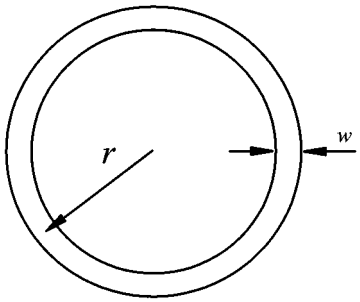

Fig. 1. Closed-loop microstrip ring resonator.

In this paper, a simple equivalent lumped-element G, L, and C circuit for closed- and open-loop ring resonators through transmission-line analysis is developed. By using the equivalent lumped elements, the unloaded Q of the closed- and open-loop rings are obtained. Two different dielectric substrates with different types of rings are used to verify the unloaded Q calculation and equivalent-circuit representation.

II. Equivalent Lumped Elements and Unloaded Q's for Closed- and Open-Loop Microstrip Ring Resonators

A. Closed-Loop Ring Resonators

Fig. 1 shows the geometry of a closed-loop microstrip ring resonator. The simple equations of the ring are given by

$$2\pi r = n\lambda_g \tag{1a}$$

$$f_o = \frac{nc}{2\pi r\sqrt{\varepsilon_{r\text{eff}}}} \tag{1b}$$

where $\lambda_g$is the guided wavelength, r is the mean radius of the ring, n is the mode number, f_o is the resonant frequency, c is the speed of light in free space, and $\varepsilon_{r\text{eff}}$ is the static effective relative dielectric constant. Observing this structure, if the width of the ring is narrow, then the ring might have the same dispersion characteristics as a transmission-line resonator [11]. Therefore, the ring resonator can be a closed-loop transmission line and can be analyzed by a transmission-line model [5].

Fig. 2(a) illustrates the one-port network of the ring and its equivalent circuit. Inspecting Fig. 2(a), the equivalent input impedance of the ring is not easily derived from the one-port network. Another approach using the two-port network is shown in Fig. 2(b) with an open circuit at port 2 ($i_2 = 0$) to model the one-port network and find the equivalent input

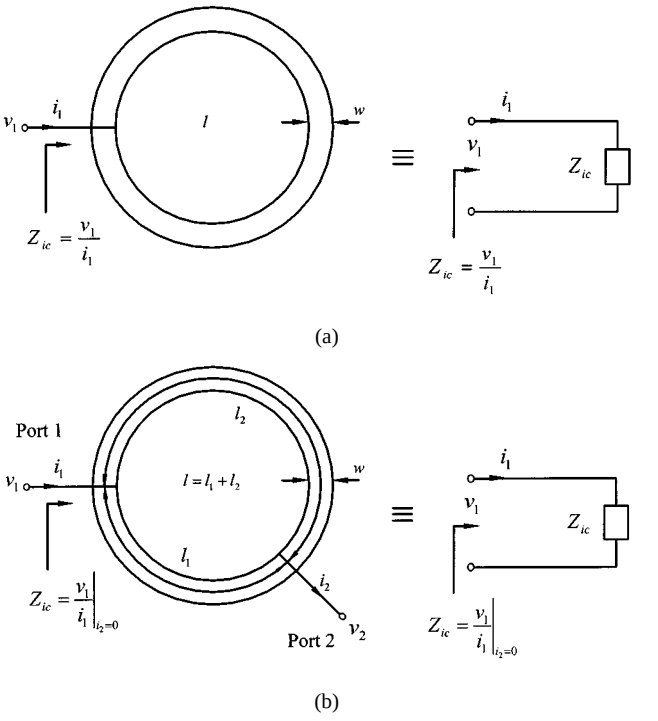

Fig. 2. Input impedance of: (a) one-port network and (b) two-port network of the closed-loop ring resonator.

impedance through $ABCD$ and Y-parameter matrix operations [11].

As seen in Fig. 2(b), the mean circumference $l = \lambda_g = 2\pi r$ for the fundamental mode $n = 1$ is divided by input and output ports on arbitrary positions of the ring with two sections l_1 and l_2. The two sections form a parallel circuit. For this parallel circuit, a transmission-line $ABCD$ matrix is utilized to find each section parameters. The $ABCD$ matrix of the individual transmission-line lengths l_1 and l_2 is given as follows:

$$\begin{bmatrix} A & B \\ C & D \end{bmatrix}_{1,2} = \begin{bmatrix} \cosh(\gamma l_{1,2}) & Z_o \sinh(\gamma l_{1,2}) \\ Y_o \sinh(\gamma l_{1,2}) & \cosh(\gamma l_{1,2}) \end{bmatrix}, \quad \gamma = \alpha + j\beta \tag{2}$$

where subscripts 1 and 2 correspond to the transmission lines l_1 and l_2, respectively, $Z_o = 1/Y_o$ is the characteristic impedance of the microstrip ring resonator, γ is the complex propagation constant, α is the attenuation constant, and β is the phase constant.

The overall Y-parameters converted from the $ABCD$ matrix in (2) for the parallel circuit are given by

$$\begin{bmatrix} Y_{11} & Y_{12} \\ Y_{12} & Y_{22} \end{bmatrix} = \begin{bmatrix} Y_o[\coth(\gamma l_1) + \coth(\gamma l_2)] & -Y_o[\operatorname{csch}(\gamma l_1) + \operatorname{csch}(\gamma l_2)] \\ -Y_o[\operatorname{csch}(\gamma l_1) + \operatorname{csch}(\gamma l_2)] & Y_o[\coth(\gamma l_1) + \coth(\gamma l_2)] \end{bmatrix} \tag{3}$$

By setting i_2 to zero, the input impedance Z_{ic} of the closed-loop ring in Fig. 2(b) can be found as follows:

$$Z_{ic} = \left.\frac{v_1}{i_1}\right|_{i_2=0} = \frac{Z_o}{2} \frac{\sinh(\gamma l)}{\cosh(\gamma l) - 1}. \tag{4}$$

Letting $l_g = l/2 = \lambda_g/2$, (4) can be rewritten as

$$Z_{ic} = \frac{Z_o}{2} \frac{1 + j\tanh(\alpha l_g)\tan(\beta l_g)}{\tanh(\alpha l_g) + j\tan(\beta l_g)}. \tag{5}$$

In most practical cases, transmission lines have small loss so that the attenuation term can be assumed that $\alpha l_g \ll 1$, and then $\tanh(\alpha l_g) \approx \alpha l_g$. Considering the βl_g term and letting the angular frequency $\omega = \omega_o + \Delta\omega$, where ω_o is the resonant angular frequency and $\Delta\omega$ is small

$$\beta l_g = \omega_o l_g / v_p + \Delta\omega l_g / v_p \tag{6}$$

where v_p is the phase velocity of the transmission line. When a resonance occurs, $\omega = \omega_o$ and $l_g = \lambda_g/2 = \pi v_p/\omega_o$. Thus, (6) can be rewritten as

$$\beta l_g = \pi + \pi\Delta\omega/\omega_o \tag{7a}$$

and

$$\tanh(\beta l_g) \approx \pi\Delta\omega/\omega_o. \tag{7b}$$

Using these results, the input impedance Z_{ic} can be approximated as

$$Z_{ic} \cong \frac{Z_o}{2} \frac{1 + j\alpha l_g \pi\Delta\omega/\omega_o}{\alpha l_g + \pi\Delta\omega/\omega_o}. \tag{8}$$

Since $\alpha l_g \pi\Delta\omega/\omega_o \ll 1$, Z_{ic} can be rewritten as

$$Z_{ic} \cong \frac{Z_o/2\alpha l_g}{1 + j\pi\Delta\omega/\alpha l_g \omega_o}. \tag{9}$$

For a general parallel GLC circuit, the input impedance is [13]

$$Z_i = \frac{1}{G + 2j\Delta\omega C}. \tag{10}$$

Comparing (9) with (10), the input impedance of the closed-loop ring resonator has the same form as that of a parallel GLC circuit. Therefore, the conductance of the equivalent circuit of the ring is

$$G_c = 2\alpha l_g / Z_o = \alpha\lambda_g / Z_o \tag{11a}$$

and the capacitance of the equivalent circuit of the ring is

$$C_c = \pi / Z_o \omega_o. \tag{11b}$$

The inductance of the equivalent circuit of the ring can be derived from $\omega_o = 1/\sqrt{L_c C_c}$ and is given by

$$L_c = 1/\omega_o^2 C_c \tag{11c}$$

where G_c, L_c, and C_c stand for the equivalent conductance, inductance, and capacitance of the closed-loop ring resonator. Fig. 3 shows the equivalent lumped-element circuit of the ring in terms of G_c, L_c, and C_c. Moreover, the unloaded Q of the ring resonator can be found from (11), and the unloaded Q is

$$Q_{uc} = \omega_o C_c / G_c = \pi / \alpha\lambda_g. \tag{12}$$

For a square ring resonator, as shown in Fig. 4, the equivalent G_c, L_c, C_c, and unloaded Q can be derived by the same procedures as above. Through the derivations, it can be found that the

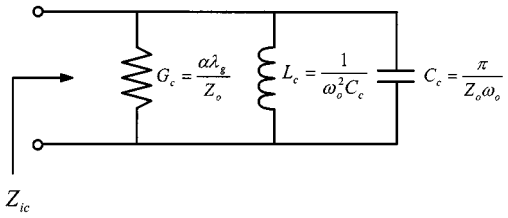

Fig. 3. Equivalent elements G_c, L_c, and C_c of the closed-loop ring resonator.

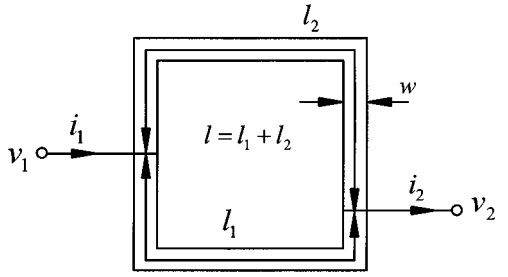

Fig. 4. Transmission-line model of the closed-loop square ring resonator.

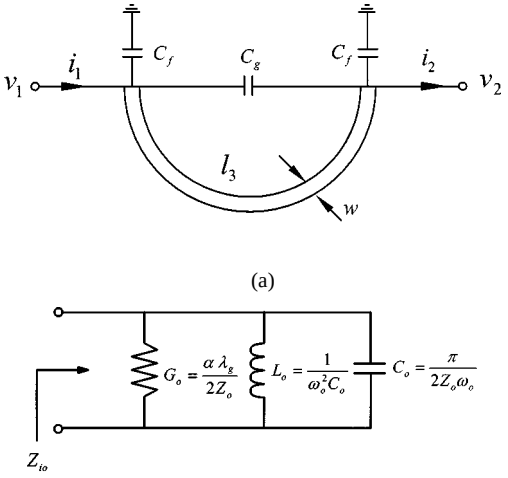

Fig. 5. Transmission-line model of: (a) the open-loop ring resonator and (b) its equivalent elements G_o, L_o, and C_o.

equivalent G_c, L_c, C_c, and unloaded Q of the square ring resonator is the same as that of the annular ring resonator in Fig. 2.

B. Open-Loop Ring Resonators

Fig. 5(a) illustrates the configuration of an open-circuited $\lambda_g/2$ microstrip ring resonator. As seen in Fig. 5(a), l_3 is the physical length of the ring, C_g is the gap capacitance, and C_f is the fringe capacitance caused by fringe field at the both ends of the ring. The fringe capacitance can be replaced by an equivalent length Δl [14]. Considering the open-end effect, the equivalent length of the ring is $l_3 + 2\Delta l = \lambda_g/2 = l_g$ for the fundamental mode.

In Fig. 5(a), the parallel circuit split by input and output ports is composed of the gap capacitor C_g and the ring resonator. Furthermore, the $ABCD$ matrix of the individual element of C_g and the ring can be expressed as follows:

$$\begin{bmatrix} A & B \\ C & D \end{bmatrix}_{C_g} = \begin{bmatrix} 1 & 1/Y_g \\ 0 & 1 \end{bmatrix} \tag{13}$$

$$\begin{bmatrix} A & B \\ C & D \end{bmatrix}_{\text{open}} = \begin{bmatrix} \cosh(\gamma l_g) & Z_o \sinh(\gamma l_g) \\ Y_o \sinh(\gamma l_g) & \cosh(\gamma l_g) \end{bmatrix} \tag{14}$$

where subscripts C_g and *open* are for the gap capacitor and the open-loop ring resonator, respectively, $Y_g = j\omega C_g$ is the admittance of C_g, $Z_o = 1/Y_o$ is the characteristic impedance of the ring.

The overall Y parameters converted from the $ABCD$ matrix in (13) and (14) for the parallel ring circuit are given by

$$\begin{bmatrix} Y_{11} & Y_{12} \\ Y_{21} & Y_{22} \end{bmatrix} = \begin{bmatrix} Y_g + Y_o \coth(\gamma l_g) & -Y_g - Y_o \operatorname{csc} h(\gamma l_g) \\ -Y_g - Y_o \operatorname{csc} h(\gamma l_g) & Y_g + Y_o \coth(\gamma l_g) \end{bmatrix}. \tag{15}$$

Observing the two-port network shown in Fig. 5(a), the input impedance of the ring can be calculated by setting output current to zero. In this condition, the input impedance can be written as

$$Z_{io} = \left.\frac{v_1}{i_1}\right|_{i_2=0} = \frac{Y_o \cosh(\gamma l_g) + Y_g \sinh(\gamma l_g)}{Y_o^2 \sinh(\gamma l_g) + 2Y_o Y_g \left[\cosh(\gamma l_g) - 1\right]}. \tag{16}$$

If the gap size between two open ends of the ring is large, then the effect of the gap capacitor C_g for the ring can be ignored [15]. This implies $Y_g \approx 0$. Therefore, the input impedance Z_{io} of the open-loop ring can be approximated as

$$Z_{io} \cong Z_o \frac{1 + j\tanh(\alpha l_g)\tan(\beta l_g)}{\tanh(\alpha l_g) + j\tan(\beta l_g)}. \tag{17}$$

Also, using the same assumptions and derivations for αl_g and βl_g as in Section II-A, the input impedance can be obtained by

$$Z_{io} = \frac{Z_o/\alpha l_g}{1 + j\pi\Delta\omega/\alpha l_g \omega_o}. \tag{18}$$

Comparing (18) with (10), the input impedance of the ring has the same form as that of a parallel GLC circuit. Thus, the conductance, capacitance, and inductance of the equivalent circuit of the ring are

$$G_o = \alpha\lambda_g/2Z_o \quad C_o = \pi/2Z_o\omega_o \quad L_o = 1/\omega_o^2 C_o. \tag{19}$$

The equivalent circuit in terms of G_o, L_o, and C_o is shown in Fig. 5(b). Moreover, the unloaded Q of the ring is given by

$$Q_{uo} = \omega_o C_o/G_o = \pi/\alpha\lambda_g. \tag{20}$$

Fig. 6 illustrates an U-shaped open-loop ring. Also, following the same derivations used in this section, the equivalent lumped elements G_o, L_o, C_o, and unloaded Q of the U-shaped ring resonator can be found to be identical to those of the open-loop ring resonator with the curvature effect.

Inspecting the equivalent conductances, capacitances, and inductances of the closed- and open-loop ring resonators from

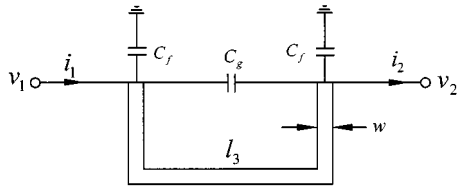

Fig. 6. Transmission-line model of the U-shaped open-loop ring resonator.

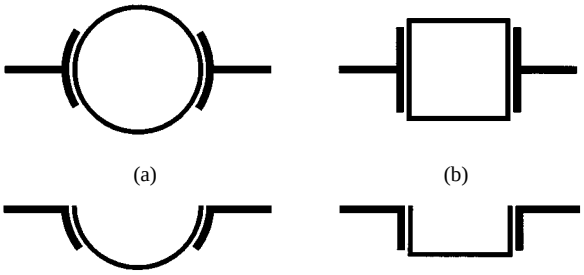

Fig. 7. Layouts of the: (a) annular, (b) square, (c) open-loop with the curvature effect, and (d) U-shaped open-loop ring resonators.

(11) and (19), the relations of the equivalent lumped elements GLC between these two rings can be found as follows:

$$G_c = 2G_o \text{ for the same attenuation constant} \tag{21a}$$
$$C_c = 2C_o$$
$$L_c = L_o/2. \tag{21b}$$

In addition, observing (12) and (20), the unloaded Q of the closed- and open-loop ring resonators are equal, namely,

$$Q_{uc} = Q_{uo} \text{for the same attenuation constant.} \tag{22}$$

Equations (21a) and (22) sustain for the same losses condition of the closed- and open-loop ring resonator. In practice, the total losses for the closed- and open-loop ring resonator are not the same. In addition to the dielectric and conductor losses, the open-loop ring resonator has a radiation loss caused by the open ends [16]. Thus, total losses of the open-loop ring are larger than that of the closed-loop ring. Under this condition, (21a) and (22) should be rewritten as follows:

$$Q_{uc} > Q_{uo} \text{ and } G_c < 2G_o. \tag{23}$$

III. Calculated and Measured Unloaded Q's and Equivalent Lumped Elements for Ring Resonators

A. Calculated Method

The attenuation constant of a microstrip line is given as follows [17]:

$$\alpha = \alpha_d + \alpha_c \tag{24}$$

where α_d and α_c are dielectric and conductor attenuation constants, respectively. The dielectric attenuation constant is given by

$$\alpha_d = 27.3 \frac{\varepsilon_r}{\varepsilon_r - 1} \frac{\varepsilon_{\text{reff}} - 1}{\sqrt{\varepsilon_{\text{reff}}}} \frac{\tan\delta}{\lambda_0} \text{ dB/unit length} \tag{25}$$

TABLE I
Unloaded Q's for the Parameters: $\varepsilon_r = 2.33$, $h = 10$ mil, $t = 0.7$ mil, and $w = 0.567$ mm for a 60-Ω Line, $\Delta = 1.397$ μm Surface Roughness, and $\lambda_g = 108.398$ mm

Resonators	Annular Ring	Open-loop Ring with the curvature effect	Square Ring	U-shaped open-loop Ring
Designed Resonant Frequency (GHz)	2	2	2	2
Measured Resonant Frequency (GHz)	1.963	1.964	1.977	1.983
Measured Insertion Loss L_{meas} (dB)	32.66	31.33	32.3	33.12
Measured 3dB Bandwidth $BW_{3dB,meas}$ (MHz)	19	19.5	19	19.5
Measured Loaded Q	103.32	100.72	104.05	101.69
Measured Unloaded Q	105.78	103.53	106.64	103.98
Calculated Unloaded Q	103.35	102.41	103.35	102.41

where ε_r is the relative dielectric constant, $\tan\delta$ is the loss tangent, and λ_0 is the wavelength in free space. If operation frequency is larger than dispersion frequency [12]

$$f_d \text{ (GHz)} = 0.3 \sqrt{\frac{Z_o}{h\sqrt{\varepsilon_r - 1}}} \tag{26}$$

where h is the substrate thickness in centimeters, then (25) has to include the effects of dispersion [18] as follows:

$$\alpha_d = 27.3 \frac{\varepsilon_r}{\varepsilon_r - 1} \frac{\varepsilon_{\text{reff}}(f) - 1}{\sqrt{\varepsilon_{\text{reff}}(f)}} \frac{\tan\delta}{\lambda_0}. \tag{27}$$

The conductor attenuation constant α_c can be approximately expressed as [17]

$$w/h \le 1/2\pi$$
$$\alpha_c = \frac{8.68 R_{s1} M}{2\pi Z_o h} \left(1 + \frac{h}{w_{\text{eff}}} + \frac{hU}{\pi w_{\text{eff}}}\right) \text{ dB/unit length} \tag{28a}$$

$$1/2\pi \le w/h \le 2$$
$$\alpha_c = \frac{8.68 R_{s1} M}{2\pi Z_o h} \left(1 + \frac{h}{w_{\text{eff}}} + \frac{hV}{\pi w_{\text{eff}}}\right) \text{ dB/unit length} \tag{28b}$$

TABLE II
EQUIVALENT ELEMENTS FOR THE PARAMETERS: $\varepsilon_r = 2.33$, $h = 10$ mil, $t = 0.7$ mil, AND $w = 0.567$ mm FOR A 60-Ω LINE, $\Delta = 1.397$ μm SURFACE ROUGHNESS, AND $\lambda_g = 108.398$ mm

Resonators	Annular Ring	Open-loop Ring with the curvature effect	Square Ring	U-shaped open-loop Ring
Calculated α (dB/mm)	2.45×10^{-3}	2.43×10^{-3}	2.45×10^{-3}	2.43×10^{-3}
Calculated Resistor G (mS)	0.508	0.256	0.508	0.256
Calculated Capacitor C (pF)	4.17	2.08	4.17	2.08
Calculated Inductor L (nH)	1.52	3.04	1.52	3.04
Measured α_{meas} (dB/mm)	2.38×10^{-3}	2.43×10^{-3}	2.36×10^{-3}	2.42×10^{-3}
Measured Resistor G (mS)	0.495	0.253	0.49	0.252
Measured Capacitor C (pF)	4.25	2.12	4.22	2.1
Measured Inductor L (nH)	1.55	3.1	1.54	3.07

TABLE III
UNLOADED QS FOR THE PARAMETERS: $\varepsilon_r = 10.2$, $h = 10$ mil, $t = 0.7$ mil, AND $w = 0.589$ mm FOR A 30-Ω LINE, $\Delta = 1.397$ μm SURFACE ROUGHNESS, AND $\lambda_g = 55.295$ mm

Resonators	Annular Ring	Open-loop Ring with the curvature effect	Square Ring	U-shaped open-loop Ring
Designed Resonant Frequency (GHz)	2	2	2	2
Actual Resonant Frequency (GHz)	1.974	1.968	2.03	2.03
Measured Insertion Loss L_{meas} (dB)	35.83	35.48	35.48	33.4
Measured 3dB Bandwidth $BW_{3dB,meas}$ (MHz)	20.5	21	20.5	21
Measured Loaded Q	96.29	95.36	97.71	95.38
Measured Unloaded Q	97.87	96.99	99.38	97.46
Calculated Unloaded Q	93.65	93.21	93.65	93.21

$$w/h \geq 2$$

$$\alpha_c = \frac{8.68R_{s1}}{2\pi Z_o h}\left[\frac{w_{\text{eff}}}{h} + \frac{w_{\text{eff}}/\pi h}{\frac{w_{\text{eff}}}{2h}+0.94}\right] \times \left(1 + \frac{h}{w_{\text{eff}}} + \frac{hV}{\pi w_{\text{eff}}}\right) \times \left\{\frac{w_{\text{eff}}}{h} + \frac{2}{\pi}\ln\left[2\pi e\left(\frac{w_{\text{eff}}}{2h}+0.94\right)\right]\right\}^{-2} \text{ dB/unit length} \quad (28c)$$

with

$$M = 1 - \left(\frac{w_{\text{eff}}}{4h}\right)^2$$

$$U = \ln\frac{4\pi w}{t} + \frac{t}{w}$$

$$V = \ln\frac{2h}{t} + \frac{t}{w}$$

$$R_{s1} = R_s\left\{1 + \frac{2}{\pi}\tan^{-1}\left[1.4\left(\frac{\Delta}{\delta_s}\right)^2\right]\right\}$$

and

$$R_s = \sqrt{\frac{\pi f \mu_0}{\sigma}}$$

[19] where R_{s1} is the surface-roughness resistance of the conductor, R_s is the surface resistance of the conductor, Δ is the surface roughness, $\delta_s = 1/R_s\sigma$ is the skin depth, σ is the conductivity of the microstrip line, f is the frequency, μ_0 is the permeability of free space, t is the microstrip thickness, and w is the width of the microstrip line. The effective width w_{eff} can be found in [20]. The unloaded Q of the closed-loop ring can be calculated by

$$1/Q_{uc} = 1/Q_d + 1/Q_c \quad (29)$$

where $Q_d = \pi/\alpha_d\lambda_g$ is the Q-factor caused by the dielectric loss of the ring and $Q_c = \pi/\alpha_c\lambda_g$ is the Q-factor caused by the conductor loss of the ring. The attenuation constant of the fundamental-mode closed-loop ring is

$$\alpha_{ca} = \alpha_d + \alpha_c \text{ Np/unit length.} \quad (30)$$

The radiation loss caused by open ends of the open-loop ring resonator in terms of radiation quality factor is [16]

$$Q_r = \frac{Z_o}{480(h/\lambda_0)^2 F} \quad (31)$$

where

$$F = \frac{\varepsilon_{\text{reff}}(f)+1}{\varepsilon_{\text{reff}}(f)} - \frac{[\varepsilon_{\text{reff}}-1]^2}{2[\varepsilon_{\text{reff}}(f)]^{3/2}}\ln\left[\frac{\sqrt{\varepsilon_{\text{reff}}(f)}+1}{\sqrt{\varepsilon_{\text{reff}}(f)}-1}\right].$$

TABLE IV
EQUIVALENT ELEMENTS FOR THE PARAMETERS: $\varepsilon_r = 10.2$, $h = 10$ mil, $t = 0.7$ mil, AND $w = 0.589$ mm FOR A 30-Ω LINE, $\Delta = 1.397$ μm SURFACE ROUGHNESS, AND $\lambda_g = 55.295$ mm

Resonators	Annular Ring	Open-loop Ring with the curvature effect	Square Ring	U-shaped open-loop Ring
Calculated α (dB/mm)	5.29×10^{-3}	5.27×10^{-3}	5.29×10^{-3}	5.27×10^{-3}
Calculated Resistor G (mS)	1.12	0.56	1.12	0.56
Calculated Capacitor C (pF)	8.33	4.17	8.33	4.17
Calculated Inductor L (nH)	0.76	1.52	0.76	1.52
Measured α_{meas} (dB/mm)	5.04×10^{-3}	5.09×10^{-3}	4.97×10^{-3}	5.06×10^{-3}
Measured Resistor G (mS)	1.06	0.54	1.05	0.54
Measured Capacitor C (pF)	8.44	4.23	8.21	4.11
Measured Inductor L (nH)	0.77	1.54	0.75	1.5

The unloaded Q of the open-loop ring can be given by

$$1/Q_{uo} = 1/Q_d + 1/Q_c + 1/Q_r. \tag{32}$$

The attenuation constant of the fundamental mode open-loop ring resonator can be derived from (20). That is

$$\alpha_{oa} = \pi/Q_{uo}\lambda_g \text{ Np/unit length}. \tag{33}$$

By using the attenuation constants in (30) and (33), the calculated equivalent lumped elements for closed- and open-loop rings can be obtained from (11) and (19).

B. Measured Method

The measured unloaded Q of a microstrip resonator can be obtained by [5]

$$Q_{u,\,\text{meas}} = \frac{Q_{L,\,\text{meas}}}{1 - 10^{-L_{\text{meas}}/20}} \tag{34}$$

where the subscript meas stands for measured data, $Q_{L,\,\text{meas}}$ is the loaded Q, and L_{meas} is the measured insertion loss in decibels of the resonator at resonance. The loaded Q is defined as

$$Q_{L,\,\text{meas}} = f_{o,\,\text{meas}}/\text{BW}_{3\,\text{dB},\,\text{meas}} \tag{35}$$

where $f_{o,\,\text{meas}}$ is the measured resonant frequency and $\text{BW}_{3\,\text{dB},\,\text{meas}}$ is the measured 3-dB bandwidth of a resonator. Also, using (12) and (20), the measured attenuation constant for the fundamental-mode closed- and open-loop rings can be given by

$$\alpha_{ca,\,\text{meas}} = \pi/Q_{cu,\,\text{meas}}\lambda_g \text{ Np/unit length} \tag{36a}$$

and

$$\alpha_{oa,\,\text{meas}} = \pi/Q_{ou,\,\text{meas}}\lambda_g \text{ Np/unit length}. \tag{36b}$$

Thus, the equivalent lumped elements G, L, and C of the closed- and open-loop rings can be found as follows:

$$\begin{aligned} G_{c,\,\text{meas}} &= \alpha_{ca,\,\text{meas}}\lambda_g/Z_o \\ C_{c,\,\text{meas}} &= \pi/Z_o\omega_{o,\,\text{meas}} \\ L_{c,\,\text{meas}} &= 1/\omega_{o,\,\text{meas}}^2 C_{c,\,\text{meas}} \end{aligned} \tag{37a}$$

$$\begin{aligned} G_{o,\,\text{meas}} &= \alpha_{oa,\,\text{meas}}\lambda_g/2Z_o \\ C_{o,\,\text{meas}} &= \pi/2Z_o\omega_{o,\,\text{meas}} \\ L_{o,\,\text{meas}} &= 1/\omega_{o,\,\text{meas}}^2 C_{o,\,\text{meas}}. \end{aligned} \tag{37b}$$

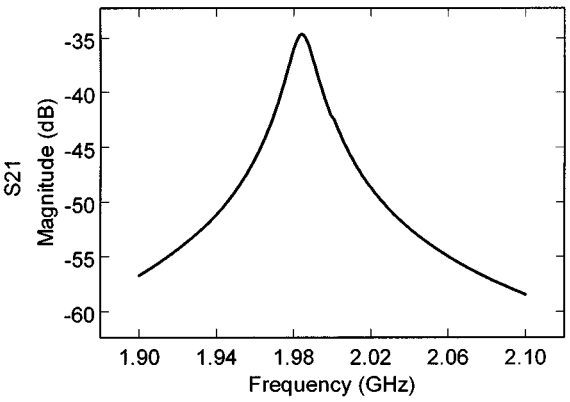

(a)

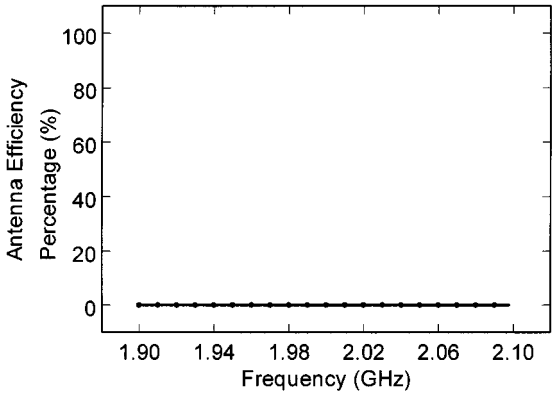

(b)

Fig. 8. Simulated: (a) $S21$ and (b) antenna efficiency for the U-shaped open-loop ring resonator.

IV. Calculated and Experimental Results

To verify the calculations presented in Section III, four configurations of the closed- and open-loop ring resonators were designed at the fundamental mode of 2 GHz. The circuits, shown in Fig. 7, were fabricated for two different dielectric constants: RT/Duriod 5870 with $\varepsilon_r = 2.33$, $h = 10$ mil, and $t = 0.7$ mil, and RT/Duriod 6010.2 with $\varepsilon_r = 10.2$, $h = 10$ mil, and $t = 0.7$ mil.

As seen in Tables I–IV, the measured unloaded Q's and equivalent lumped elements of the closed- and open-loop rings show good agreement with each other. The differences between the measured and calculated results are caused by measurement uncertainties and the accuracy limitations of the calculation equations. The largest difference between the measured and calculated unloaded Q shown in Table III for the closed-loop square ring resonator is 5.7%. Furthermore, an electromagnetic (EM) simulator based on an integral equation and method of moment[1] is used to investigate the radiation effect of the open-loop ring resonator fabricated with $\varepsilon_r = 2.33$ and $h = 10$ mil. Fig. 8 shows $S21$ of the U-shaped open-loop ring resonator at the fundamental resonant frequency and its antenna efficiency. Observing the result in Fig. 8(b), the antenna efficiency of the ring resonator is 0.0003% at the resonant frequency. From the results, it is found that the radiation loss contributes little to the losses of the ring circuit and insignificantly affects the unloaded Q of the ring resonator under the conditions of low resonant frequency, high characteristic impedance, and thin substrate, which can also be inspected by (31).

V. Conclusions

An equivalent lumped-element circuit representation for the closed- and open-loop ring resonators has been developed by a transmission-line analysis. Using the calculated G, L, and C element values, the unloaded Q's for both the closed- and open-loop ring resonators have been obtained. Two different dielectric constant substrates have been used to verify the unloaded Q's and the equivalent lumped elements. The measured results show good agreement with the theory. These novel expressions using the equivalent lumped elements G, L, C, and unloaded Q for the ring resonators can provide a simple way to design ring circuits.

Acknowledgment

The authors would like to thank C. Wang, Texas A&M University, College Station, for his technical assistance and C. Rodenbeck, Texas A&M University, College Station, for his helpful discussions.

References

[1] P. Troughton, "Measurement technique in microstrip," *Electron. Lett.*, vol. 5, no. 2, pp. 25–26, Jan. 1969.
[2] I. Wolff and N. Knoppik, "Microstrip resonator and dispersion measurements on microstrip lines," *Electron. Lett.*, vol. 7, no. 26, pp. 779–781, Dec. 1971.
[3] W. Hoefer and A. Chattopadhay, "Evaluation of the equivalent circuit parameters of microstrip discontinuities through perturbation of a resonant ring," *IEEE Trans. Microwave Theory Tech.*, vol. MTT-23, pp. 1067–1071, Dec. 1975.
[4] K. Chang, F. Hsu, J. Berenz, and K. Nakano, "Find optimum substrate thickness for millimeter-wave GaAs MMICs," *Microwave RF*, vol. 27, pp. 123–128, Sept. 1984.
[5] K. Chang, *Microwave Ring Circuits and Antennas*. New York: Wiley, 1996.
[6] J. S. Hong and M. J. Lancaster, "Microstrip bandpass filter using degenerate modes of a novel meander loop resonator," *IEEE Microwave Guided Wave Lett.*, vol. 5, pp. 371–372, Nov. 1995.
[7] ——, "Compact microwave elliptic function filter using novel microstrip meander open-loop resonators," *Electron. Lett.*, vol. 32, no. 6, pp. 563–564, Mar. 1996.
[8] Y. S. Wu and F. J. Rosenbaum, "Mode chart for microstrip resonators," *IEEE Trans. Microwave Theory Tech.*, vol. MTT-21, pp. 487–489, July 1973.
[9] K. Chang, T. S. Martin, F. Wang, and J. L. Klein, "On the study of microstrip ring and varactor-tuned circuits," *IEEE Trans. Microwave Theory Tech.*, vol. MTT-35, pp. 1288–1295, Dec. 1987.
[10] G. K. Gopalakrishnan and K. Chang, "Bandpass characteristics of split-modes in asymmetric ring resonators," *Electron. Lett.*, vol. 26, no. 12, pp. 774–775, June 1990.
[11] C. C. Yu and K. Chang, "Transmission-line analysis of a capacitively coupled microstrip-ring resonator," *IEEE Trans. Microwave Theory Tech.*, vol. 45, pp. 2018–2024, Nov. 1997.
[12] G. Gonzalez, *Microwave Transistor Amplifiers Analysis and Design*, 2nd ed. Englewood Cliffs, NJ: Prentice-Hall, 1997, pp. 1–4, 148–149.
[13] D. M. Pozar, *Microwave Engineering*, 2nd ed. New York: Wiley, 1998, pp. 303–306.
[14] R. Garg and I. J. Bahl, "Microstrip discontinuities," *Int. J. Electron.*, vol. 45, pp. 81–87, July 1978.
[15] V. K. Tripathi and I. Wolff, "Perturbation analysis and design equations for open- and closed-ring microstrip resonators," *IEEE Trans. Microwave Theory Tech.*, vol. MTT-32, pp. 405–409, Apr. 1984.
[16] E. Belohoubek and E. Denlinger, "Loss considerations for microstrip resonators," *IEEE Trans. Microwave Theory Tech.*, vol. MTT-23, pp. 522–526, June 1975.
[17] R. A. Pucel, D. J. Massé, and C. P. Hartwig, "Losses in microstrip," *IEEE Trans. Microwave Theory Tech.*, vol. MTT-16, pp. 342–350, June 1968.
[18] M. Kobayashi, "A dispersion formula satisfying recent requirements in microstrip CAD," *IEEE Trans. Microwave Theory Tech.*, vol. 36, pp. 1246–1250, Aug. 1988.
[19] E. Hammerstad and O. Jensen, "Accurate models for microstrip computer-aided design," in *IEEE MTT-S Int. Microwave Symp. Dig.*, 1980, pp. 407–409.
[20] I. J. Bahl and R. Garg, "Simple and accurate formulas for microstrip with finite strip thickness," *Proc. IEEE*, vol. 65, pp. 1611–1612, Nov. 1977.

[1] IE3D Version 6.1, Zeland Software Inc., Fremont, CA, Aug. 1998.

Lung-Hwa Hsieh (S'01) was born in Panchiao, Taiwan, R.O.C., in 1969. He received the B.S. degree in electrical engineering from the Chung Yuan Christian University, Chungli, Taiwan, R.O.C., in 1991, the M.S. degree in electrical engineering from the National Taiwan University of Science and Technology, Taipei, Taiwan, R.O.C., in 1993, and is currently working toward the Ph.D. degree in electrical engineering at Texas A&M University, College Station.

From 1995 to 1998, he was a Senior Design Engineer at General Instrument, Taipei, Taiwan, R.O.C., where he was involved in RF video and audio circuit design. Since 2000, he has been a Research Assistant in the Department of Electrical Engineering, Texas A&M University, College Station. His research interests include microwave integrated circuits and devices.

Kai Chang (S'75–M'76–SM'85–F'91) received the B.S.E.E. degree from the National Taiwan University, Taipei, Taiwan, R.O.C., in 1970, the M.S. degree from the State University of New York at Stony Brook, in 1972, and the Ph.D. degree from The University of Michigan at Ann Arbor, in 1976.

From 1972 to 1976, he was a Research Assistant with the Microwave Solid-State Circuits Group, Cooley Electronics Laboratory, The University of Michigan at Ann Arbor. From 1976 to 1978, he was with Shared Applications Inc., Ann Arbor, MI, where he was involved with computer simulation of microwave circuits and microwave tubes. From 1978 to 1981, he was with the Electron Dynamics Division, Hughes Aircraft Company, Torrance, CA, where he was involved in the research and development of millimeter-wave solid-state devices and circuits, power combiners, oscillators, and transmitters. From 1981 to 1985, he was a Section Head with TRW Electronics and Defense, Redondo Beach, CA, where he developed state-of-the-art millimeter-wave integrated circuits and subsystems including mixers, voltage-controlled oscillators (VCOs), transmitters, amplifiers, modulators, upconverters, switches, multipliers, receivers, and transceivers. In August 1985, he joined the Electrical Engineering Department, Texas A&M University, as an Associate Professor, and then became a Professor in 1988. In January 1990, he was appointed E-Systems Endowed Professor of Electrical Engineering. His current interests are in microwave and millimeter-wave devices and circuits, microwave integrated circuits, integrated antennas, wide-band and active antennas, phased arrays, microwave power transmission, and microwave optical interactions. He has authored or co-authored several books, including *Microwave Solid-State Circuits and Applications* (New York: Wiley, 1994), *Microwave Ring Circuits and Antennas* (New York: Wiley, 1996), *Integrated Active Antennas and Spatial Power Combining* (New York: Wiley, 1996), and *RF and Microwave Wireless Systems* (New York: Wiley, 2000). He was the editor of the four-volume *Handbook of Microwave and Optical Components* (New York: Wiley, 1989, 1990). He is the Editor of *Microwave and Optical Technology Letters* and the Wiley Book Series in "Microwave and Optical Engineering." He has authored or co-authored over 350 technical papers and several book chapters in the areas of microwave and millimeter-wave devices, circuits, and antennas.

Dr. Chang was the recipient of the 1984 Special Achievement Award presented by TRW, the 1988 Halliburton Professor Award, the 1989 Distinguished Teaching Award, the 1992 Distinguished Research Award, and the 1996 TEES Fellow Award presented by the Texas A&M University.